

on the extended Press–Schechter theory (see Salvadori et al. 2007 for more details). The evolution of gas and stars is then followed along each hierarchical tree by assuming that (1) the initial gas content of DM haloes is equal to the universal cosmological value $(\Omega_b/\Omega_m)M_h$, where M_h is the DM halo mass and $\Omega_b(\Omega_m)$ is the baryonic (DM) density parameter; (2) at any redshift, there exists a minimum halo mass to form stars, $M_{\text{sf}}(z)$, whose evolution accounts for the suppression of star formation (SF) in progressively more massive objects due to radiative feedback effects (see fig. 1 of Salvadori & Ferrara 2009); (3) the gradual accretion of cold gas, M_c , into newly virializing haloes is regulated by a numerically calibrated infall rate (Kereš et al. 2005); (4) the SF rate, \dot{M}_* , is proportional to the mass of cold gas inside each galaxy, $\dot{M}_* = \epsilon_* M_c / t_{\text{ff}}$, where ϵ_* is the SF efficiency and t_{ff} the halo free fall time; (5) in haloes with a virial temperature, $T_{\text{vir}} < 10^4$ K (minihaloes), the SF efficiency is reduced as $\epsilon = \epsilon_* [1 + (T_{\text{vir}}/2 \times 10^4 \text{ K})^{-3}]^{-1}$ due to ineffective cooling by H_2 molecules. The chemical enrichment of gas, both in the proto-Galactic haloes and in the MW environment, is followed simultaneously by taking into account the mass-dependent stellar evolutionary time-scales and the effects of mechanical feedback due to supernova (SN) energy deposition (see Salvadori et al. 2008 for more details).

The two free parameters of the model (SF and wind efficiencies) are calibrated by reproducing the global properties of the MW (stellar/gas mass and metallicity) and the metallicity distribution function (MDF) of Galactic halo stars (Salvadori et al. 2007, 2008); $M_{\text{sf}}(z)$ is fixed by matching the observed iron–luminosity relation for dwarf spheroidal galaxies (Salvadori & Ferrara 2009). They are assumed to be the same for all progenitors in the hierarchical tree.

3 IDENTIFYING LAES

By using GAMETE, we obtain the total halo/stellar/gas masses (M_h , M_* , M_g), the instantaneous SF rate (\dot{M}_*), the mass-weighted stellar metallicity (Z_*) and the mass-weighted stellar age (t_*) of each MW progenitor, in each of the 80 realizations considered. These outputs are used to calculate the total intrinsic Ly α (L_α^{int}) and continuum luminosity (L_c^{int}) which include the contribution both from stellar sources and from the cooling of collisionally excited neutral hydrogen (H I) in the interstellar medium (ISM; Dayal et al. 2010a).

The intrinsic Ly α luminosity can be translated into the observed luminosity such that $L_\alpha = L_\alpha^{\text{int}} f_\alpha T_\alpha$, while the observed continuum luminosity, L_c , is expressed as $L_c = L_c^{\text{int}} f_c$. Here, $f_\alpha(f_c)$ are the fractions of Ly α (continuum) photons escaping the galaxy, undamped by the ISM dust, and T_α is the fraction of the Ly α luminosity that is transmitted through the IGM, undamped by H I.²

The main features of the model used to calculate f_c , f_α and T_α are as follows. (1) For each MW progenitor, the dust enrichment is derived by using its intrinsic properties (\dot{M}_* , t_* , M_g) and assuming Type II supernovae (SNII) to be the primary dust factories. The dust mass, M_d , is calculated including dust production due to SNII (each SN produces $0.5 M_\odot$ of dust), dust destruction with an efficiency of about 40 per cent in the region shocked to speeds of $\geq 100 \text{ km s}^{-1}$ by SNII shocks, assimilation of a homogeneous mixture of dust and gas into subsequent SF (accretion), and ejection of a homogeneous mixture of gas and dust from the galaxy due to SNII. (2) Following the calculations presented in Dayal et al. (2010c) for high- z

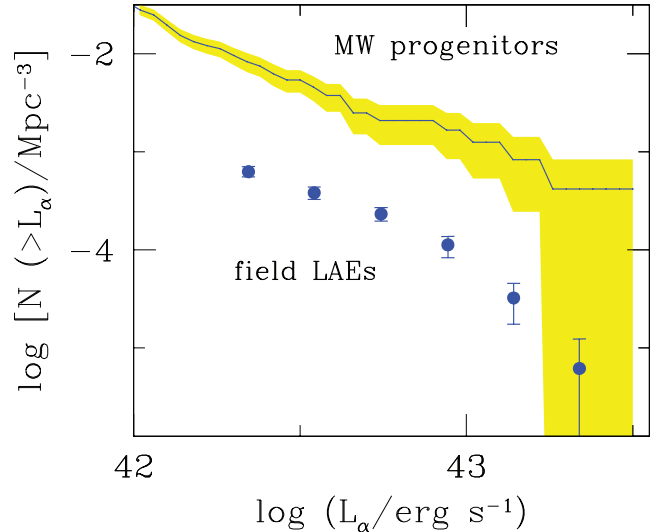


Figure 1. Cumulative Ly α LF at redshift $z \approx 5.7$. The solid line shows the mean Ly α LF of the MW progenitors averaged over 80 realizations of the merger tree; the dashed area represents the $\pm 1\sigma$ spread among different realizations. For comparison only, we show (points) the field LAE LF (Shimasaku et al. 2006).

LAEs, the dust distribution radius, r_d , is taken to scale with the gas distribution scale, r_g , such that $r_d \sim 0.5r_g$.³ (3) f_c is calculated assuming a slab-like dust distribution and we use $f_\alpha = 1.3f_c$, as inferred for LAEs at $z \approx 6$. (4) T_α is calculated using the mean photoionization rate predicted by the Early Reionization Model (ERM; reionization ends at $z \approx 7$) of Gallerani et al. (2008), according to which the neutral hydrogen fraction $\chi_{\text{HI}} = 7 \times 10^{-5}$ at $z \approx 5.7$. Complete details of these calculations can be found in Dayal et al. (2010a,c).

Progenitors are then identified as LAEs based on the currently used observational criterion: $L_\alpha \geq 10^{42} \text{ erg s}^{-1}$ and the observed equivalent width (EW), $L_\alpha/L_c \geq 20 \text{ \AA}$. We use a comoving volume of the MW environment (30 Mpc^3) to calculate the number density of the progenitors visible as LAEs and the observed LAE luminosity function (LF), shown in Fig. 1.

4 RESULTS

We start by comparing the number density of field LAEs observed at $z \approx 5.7$ with the average LF of the MW progenitors at the same epoch (Fig. 1). The number density of MW progenitors decreases with increasing Ly α luminosity, reflecting the higher abundance of the least massive/luminous objects in Λ cold dark matter models. The MW progenitors cover the entire range of observed Ly α luminosities, $L_\alpha = 10^{42-43.25} \text{ erg s}^{-1}$. We then conclude that *among the LAEs observed at $z \approx 5.7$, there are progenitors of MW-like galaxies*. For any given L_α , the number density of MW progenitors is higher than the observed value because the MW environment is a high-density, biased region. As discussed in Section 5, uncertainties on the treatment of dust may also play a role.

In Fig. 2 we show the probability distribution function (PDF), P , of finding a number N_{LAEs} of LAEs in any given MW realization. The PDF has a maximum ($P = 0.42$) at $N_{\text{LAEs}} = 1$; while in any

² The continuum band (1250–1500 Å) is chosen so as to be unaffected by H I absorption.

³ The gas distribution radius is calculated as $r_g = 4.5\lambda r_{200}$, where the spin parameter $\lambda = 0.05$ (Ferrara, Pettini & Shchekinov 2000) and r_{200} is the virial radius.

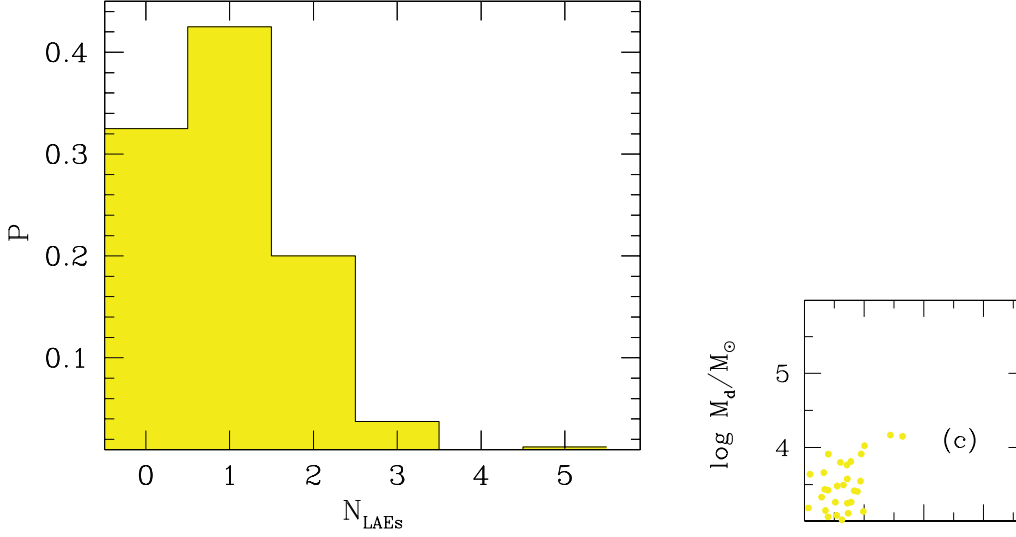


Figure 2. Probability of finding a number, N_{LAEs} , of LAEs in a single MW realization, averaged over 80 hierarchical merger histories at $z \approx 5.7$.

single MW realization, there are ≈ 50 star-forming progenitors with stellar masses $M_* \gtrsim 10^7 M_\odot$, on average only one of them would be visible as an LAE. We note that $P = 0.32$ for $N_{\text{LAEs}} = 0$, while it rapidly declines ($P < 0.2$) for $N_{\text{LAEs}} > 1$. We conclude that the MW progenitors that would be observable as LAEs at $z \approx 5.7$ are rare ($\approx 1/50$), but the probability of having *at least* one LAE in any MW hierarchical merger history is very high, $P = 68$ per cent.

Let us now consider the physical properties of the building blocks of the MW. \dot{M}_* represents the dominant physical factor to determine whether a progenitor would be visible as an LAE, since it governs the intrinsic Ly α /continuum luminosity, the dust enrichment (and hence absorption) and T_α , as both the size of the ionized region around each source and the H I ionization fraction inside it scale with \dot{M}_* (Dayal et al. 2008). This implies the existence of an SF rate threshold for MW progenitors to be visible as LAEs which is $\dot{M}_*^{\text{min}} \approx 0.9 M_\odot \text{ yr}^{-1}$ (panel a of Fig. 3). Since $\dot{M}_* \propto \dot{M}_g$ (see Section 2), such a lower limit can be translated into a threshold gas mass: $M_g^{\text{min}} \approx 8 \times 10^7 M_\odot$ (panel b). In turn, the gas content of a (proto-) galaxy is predominantly determined by the assembling history of its halo and the effects of SN (mechanical) feedback. While the most massive MW progenitors ($M_h > 10^{10} M_\odot$) display a tight M_g – M_h correlation, the least massive ones are highly scattered, reflecting the strong dispersion in the formation epoch/history of recently assembled haloes (panel b). As a consequence, *LAEs typically correspond to the most massive progenitors of the hierarchical tree*, i.e. the major branches (black points in the panels). In particular, we find that *all* haloes with $M_h \geq 10^{10} M_\odot$ (40 haloes) are LAEs. At decreasing M_h , instead, the progenitors can be visible as LAEs only by virtue of a high gas mass content or extremely young ages; there are five such objects, with $M_h \approx 10^9 M_\odot$, as seen from panel (b).

By comparing panels (b) and (c) of Fig. 3, we can see that M_d of the Galactic building blocks closely tracks M_g . Since the gas mass content of the $z \approx 5.7$ MW progenitors is reduced by ≈ 1 order of magnitude with respect to the initial cosmic value, due to gas (and dust) loss in galactic winds, their resulting dust mass is relatively small: $M_d \approx 10^{4-5.7} M_\odot$. As a consequence, all the progenitor galaxies have a colour excess $E(B-V) < 0.025$. In panel (d), we see that as expected, $E(B-V)$ increases with M_* , i.e. more massive galaxies are redder. However the trend is inverted for

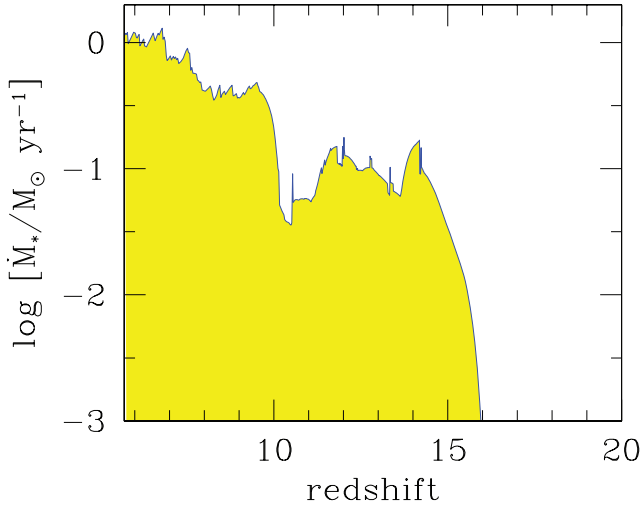


Figure 4. SFH of a typical MW progenitor identified as an LAE at $z \approx 5.7$.

In panel (f), we can see that these newly virializing galaxies are metal-poor objects, with an average stellar metallicity $Z \approx 0.016\text{--}0.044 Z_\odot$. As these galaxies host a single and extremely young stellar population, such a low Z value reflects the metallicity of the MW environment at their formation epoch, $z \approx 5.7$ (see the middle panel in fig. 1 of Salvadori et al. 2008). The more massive MW progenitors visible as LAEs, instead, are more metal rich, $Z \approx 0.3\text{--}1 Z_\odot$; their intermediate stellar populations form during a long period (see Fig. 4) and from a gas that is progressively enriched by different stellar generations.

The fact that the physical properties of the LAE progenitors obtained with our model are consistent with those inferred from the observations of field LAEs (Fig. 3) is a notable success of our model.

As mentioned above, the scatter in the LAE ages originates from different assembling and SF histories (SFH) of the MW progenitors. This can be better understood by considering the SFH of a typical⁴ MW progenitor identified as an LAE, as shown in Fig. 4. We find that since most LAEs typically correspond to the major branch, their progenitor seeds are associated with high- σ peaks of the density field virializing and starting to form stars at high redshifts ($z \approx 16$). The SF rapidly changes in time, exhibiting several bursts of different intensities and durations, which follow merging events refuelling gas for SF. During the ‘quiet’ phase of accretion, instead, SN feedback regulates SF into a more gentle regime. The duration and intensity of the peaks depend on the effectiveness of these two competitive physical processes. At high redshifts ($z > 10$), the peaks are more pronounced because (i) the frequency of major merging is higher and (ii) mechanical feedback is stronger given the shallower potential well of the hosting haloes ($M \approx 10^{8.5} M_\odot$ Salvadori et al. 2008).

We finally turn to the last question concerning the contribution of old and massive progenitors seen as LAEs to the very metal-poor stars ($[\text{Fe}/\text{H}] < -2$) observed in the MW halo. In Fig. 5, we show the fractional contribution of long-living stars from LAEs to the MDF at $z = 0$. LAEs provide > 10 per cent of the very metal-poor stars; the more massive the LAEs, the higher is the number of $[\text{Fe}/\text{H}] < -2$

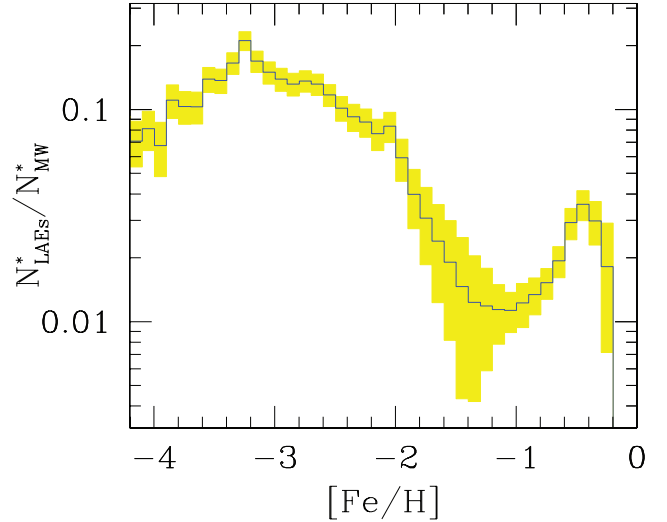


Figure 5. Fraction of LAE MW halo relic stars as a function of their iron abundance. The histogram shows the average fraction among 80 realizations of the hierarchical tree; the shaded area shows the $\pm 1\sigma$ dispersion among different realizations.

stars they contribute. This is because such metal-poor stellar fossils form at $z > 6$ in newly virializing haloes accreting pre-enriched gas out of the MW environment (see Salvadori et al. 2007, 2010). By $z \approx 5.7$, many of these premature building blocks have merged into the major branch, i.e. the LAE. Because of the gradual enrichment of the MW environment, which reaches $[\text{Fe}/\text{H}] \approx -2$ at $z \approx 5.7$ (see fig. 1 of Salvadori et al. 2008), most of $[\text{Fe}/\text{H}] > -2$ stars form at lower redshifts, $z < 5.7$, thus producing the drop at $[\text{Fe}/\text{H}] > -2$. Note also the rapid grow of $N_{\text{LAEs}}^*/N_{\text{MW}}^*$ at $[\text{Fe}/\text{H}] > -1$, which is a consequence of the self-enrichment of building blocks resulting from *internal* SN explosions.

5 CONCLUSIONS

We have linked the properties of high- z LAEs to the local Universe by coupling the semi-analytical code GAMETE to a previously developed LAE model. According to our results, the progenitors of MW-like galaxies cover a wide range of observed Ly α luminosities, $L_\alpha = 10^{39\text{--}43.25} \text{ erg s}^{-1}$, with L_α increasing with M_* (or, equivalently, M_h); hence, some of them can be observed as LAEs. In each hierarchical merger history we find that, on average, *only one* star-forming progenitor (among ≈ 50) is an LAE, usually corresponding to the major branch of the tree ($M_h \approx 10^{10} M_\odot$). Nevertheless, the probability of having *at least* one visible progenitor in any merger history is very high ($P = 68$ per cent). Interestingly, we found that the LAE candidates can also be observed as dropout galaxies since their UV magnitudes are always $M_{\text{UV}} < -18$.

On average, the identified LAE stars have intermediate ages, $t_* \approx 150\text{--}400$ Myr, and metallicities $Z \approx 0.3\text{--}1 Z_\odot$; an exception is represented by five newly formed galaxies, which are hosted by small DM haloes, $M_h \approx 10^9 M_\odot$, which are yet visible as (faint) LAEs ($L_\alpha \approx 10^{42.05} \text{ erg s}^{-1}$) by virtue of their high SF rate and extremely young stellar population, $t_* < 5$ Myr. The low metallicity of these young galaxies, $Z \approx 0.016\text{--}0.044 Z_\odot$, reflects that of the MW environment at their formation epoch. Although rare (five out of 80 LAEs), these Galactic building blocks could be even more unambiguously identified among the least luminous LAEs, due to their larger Ly α EWs, $\text{EW} = 60\text{--}130 \text{ \AA}$ with respect to those

⁴ We define as ‘typical’ an LAE whose properties match the average values: $M_h \approx 10^{10} M_\odot$, $M_g \approx 10^8 M_\odot$, $\dot{M}_* \approx 2.3 M_\odot \text{ yr}^{-1}$, $t_* \approx 230$ Myr.

($\approx 40 \text{ \AA}$) shown by older LAEs.⁵ These small and recently virialized haloes ($z_{\text{vir}} \lesssim 6$) could be the progenitors of Fornax-like dwarf spheroidal galaxies (see fig. 1 of Salvadori & Ferrara 2009). By identifying these LAEs, therefore, it would be possible to observe the most massive dSphs of the MW system just at the time of their birth.

Uncertainties remain on the treatment of dust in calculating the LF and observed properties of the MW progenitor LAEs identified here, especially at the low-luminosity end of the LF. Several aspects require additional study. As gas, metal and dust are preferentially lost from low-mass haloes, pushing the mass resolution of simulations to even lower masses would be important. Also, the amount of dust lost in SN-driven winds remains very poorly understood, an uncertainty that propagates in the evaluation of the continuum and Ly α radiation escaping from the galaxy. Finally, Ly α photons could be affected considerably by the level of dust clumping. It is unclear to what extent these effects may impact the visibility of LAEs, as discussed in e.g. Dayal et al. (2010a). Progress on these issues is expected when high-resolution FIR/sub-mm observations of LAEs with ALMA will become available in the near future (Finkelstein et al. 2009; Dayal, Hirashita & Ferrara 2010b).

ACKNOWLEDGMENT

We thank the anonymous referee for his/her positive and useful comments.

⁵ Due to the low dust mass, $f_c = f_\alpha \approx 1$ for all the progenitors we identify as LAEs; the observed EW is solely governed by T_α , which leads $\text{EW} \approx 40 \text{ \AA}$ for almost all LAEs, except those with $t_* \leq 10 \text{ Myr}$.

REFERENCES

- Cowie L. L., Hu E. M., 1998, *AJ*, 115, 1319
 Dayal P., Ferrara A., Gallerani S., 2008, *MNRAS*, 389, 1683
 Dayal P. et al., 2009, *MNRAS*, 400, 2000
 Dayal P., Ferrara A., Saro A., 2010a, *MNRAS*, 402, 1449
 Dayal P., Hirashita H., Ferrara A., 2010b, *MNRAS*, 403, 620
 Dayal P., Maselli A., Ferrara A., 2010c, preprint (arXiv:1002.0839)
 Ferrara A., Pettini M., Shchekinov Y., 2000, *MNRAS*, 319, 539
 Finkelstein S. L. et al., 2007, *ApJ*, 660, 1023
 Finkelstein S. L. et al., 2009, *MNRAS*, 393, 1174
 Gallerani S., Ferrara A., Fan X., Choudhury T. R., 2008, *MNRAS*, 386, 359
 Gawiser E. et al., 2007, *ApJ*, 671, 278
 Guaita L. et al., 2010, *ApJ*, 714, 255
 Kashikawa N. et al., 2006, *ApJ*, 648, 7
 Kereš D., Katz N., Weinberg D. H., Dave R., 2005, *MNRAS*, 363, 2
 Lai K. et al., 2007, *ApJ*, 655, 704
 Malhotra S. et al., 2005, *ApJ*, 626, 666
 Matsuda Y. et al., 2005, *ApJ*, 634, 125
 Nagamine K., Ouchi M., Springel V., Hernquist L., 2008, preprint (arXiv:0802.0228)
 Nilsson K. K. et al., 2009, *A&A*, 498, 13
 Ono Y. et al., 2010, preprint (arXiv:1004.0963)
 Ouchi M. et al., 2008, *ApJS*, 176, 301
 Pirzkal N., Malhotra S., Rhoads J. E., Xu C., 2007, *ApJ*, 667, 49
 Salvadori S., Ferrara A., 2009, *MNRAS*, 395, L6
 Salvadori S., Schneider R., Ferrara A., 2007, *MNRAS*, 381, 647
 Salvadori S., Ferrara A., Schneider R., 2008, *MNRAS*, 386, 348
 Salvadori S. et al., 2010, *MNRAS*, 401, L5
 Santos M. R., 2004, *MNRAS*, 349, 1137
 Shimasaku K. et al., 2006, *PASJ*, 58, 313
 Steidel C. C. et al., 2000, *ApJ*, 532, 170
 Taniguchi Y. et al., 2005, *PASJ*, 57, 165
 Venemans B. P. et al., 2007, *A&A*, 461, 823

This paper has been typeset from a \LaTeX file prepared by the author.